Kinetics of Release of Particulate Solutes Incorporated in Cellulosic Polymer Matrices as a Function of Solute Solubility and Polymer Swellability. II. Highly Soluble Solute

K. G. PAPADOKOSTAKI, S. G. AMARANTOS, J. H. PETROPOULOS

Institute of Physical Chemistry, Demokritos National Research Center, 153 10 Ag. Paraskevi, Athens, Greece

Received 1 July 1997; accepted 6 December 1997

ABSTRACT: The kinetics of release into water of particulate NaCl (used here as an example of a highly water-soluble solute) incorporated in a cellulose acetate (CA) matrix was investigated in correlation with the concurrent variation of the water content of the matrix. To ensure comparability with the kinetic behavior of sparingly soluble solutes reported in part I, a CA of the same composition, and identical film-forming procedures were employed. In contrast to this sparingly soluble solute behavior, deviations from $\sqrt{t}$ release kinetics and temporary osmotically induced retention of excess imbibed water were observed. Both these effects became more noticeable with decreasing salt loads. At the same time the observed release rates were far in excess of what could be expected from measurements of the NaCl transport properties of the particle-depleted matrix or what could be predicted on the basis of model calculations assuming homogeneous and instantaneously reversible osmotically induced excess water uptake. Such a marked enhancement of release rate is commonly attributed to the formation of a pore network in the particle-depleted matrix by mechanical rupture of the "walls" separating neighboring particle-containing cavities, due to osmotically induced ingress of water therein. However, it was shown that such a mechanism is unsustainable in the present context. A new, more general mechanism is proposed that can successfully account for all the salient kinetic features of the combined solute release and water absorption–desorption processes noted here. Additionally, slow molecular relaxation processes were also shown to play a significant role in the mechanism of solute release. © 1998 John Wiley & Sons, Inc. J Appl Polym Sci 69: 1275–1290, 1998

Key words: release kinetics; osmotically active agents; nonhomogeneous osmotic swelling; cellulose acetate

INTRODUCTION

In part I[1] the kinetics of release into water of sparingly water-soluble salts dispersed in hydrophobic or hydrophilic cellulosic polymer films was investigated as a function of salt load and polymer swellability. Apart from short time deviations due to some extraneous but well-understood effects, good conformity to $\sqrt{t}$ release kinetics was observed in all cases as expected theoretically[2,3] when

1. the presence of solute does not materially affect the degree of swelling of the polymer matrix and
2. either solvent penetration is fast by compari-

Correspondence to: J. H. Petropoulos (petrop@cyclades.nrcps.ariadne-t.gr).

Contract grant sponsor: European Community's Research Program on Management and Disposal of Radioactive Waste; contract grant numbers: FI1W/0026/00 and FI1W/0174/GR(TT).

Journal of Applied Polymer Science, Vol. 69, 1275–1290 (1998)
 CCC 0021-8995/98/071275-16

son with the release of solute or the loaded polymer matrix is preswollen in the solvent.

As mentioned in part I,[1] the release of water-soluble solutes from swellable polymers is generally a more complicated phenomenon. Deviations from conditions 1 and 2 may be expected to be especially noticeable in relatively hydrophobic polymer matrices, the swelling of which may be substantially enhanced by the excess water uptake induced by the osmotically active solute ("osmotic swelling").

For very fine and homogeneous solute dispersions in matrices consisting of relatively flexible polymer chains, it is possible to model, in a reasonably realistic manner, the effect on release kinetics of the aforementioned deviations from conditions 1 and 2.

In particular, assuming polymer swelling (including osmotic swelling) to be homogeneous and instantaneously reversible, so that the properties of the matrix revert to those of the neat polymer upon solute depletion and solvent transport obeys Fickian diffusion kinetics, unidimensional solvent and solute transport were described in a previous article[3] by

$$\frac{\partial C_W}{\partial t} = \frac{\partial}{\partial x}\left(D_W S_W \frac{\partial a_W}{\partial x}\right) \tag{1}$$

$$\frac{\partial C_N}{\partial t} = \frac{\partial}{\partial x}\left(D_N S_N \frac{\partial a_N}{\partial x}\right) \tag{2}$$

In eqs. (1) and (2), solvent and solute are denoted by subscripts W and N, respectively; C and a represent, respectively, concentration and activity of the relevant species in the polymer matrix (C_N includes both dispersed and dissolved solute); D and S are the corresponding "thermodynamic" diffusion and solubility coefficients, respectively; and $0 \leq x \leq l$ and t are the relevant space and time coordinates, respectively, assuming the polymer matrix to be in the form of a film of half-thickness l. In terms of activity (instead of concentration) gradients, the above formulation permits a physically realistic representation of the thermodynamic and kinetic interactions of the diffusing species in terms of the simple functional dependences of the relevant diffusion and solubility coefficients on solvent and/or solute concentration.

The sorption behavior of the solvent is represented by[3]

$$S_W = C_W/a_W = (K_{W1} + K_{W2}a_W)(1 + K_{W3}C_N) \tag{3}$$

where a_W is identified with the relative vapor pressure (neglecting vapor nonideality effects) at equilibrium with C_W; and K_{W1}, K_{W2}, and K_{W3} are constant parameters respectively describing the Henry law absorption at low C_W, the (positive) deviation from Henry's law that commonly characterizes polymer–solvent systems at higher C_W, and the enhancement of solvent uptake due to the osmotic activity of the solute. For the neat polymer swollen in bulk solvent $C_W = C_W^0 = S_W$ ($a_W = 1$, $C_N = 0$).

For the sorption of solute by the hydrated polymer matrix, we have[3]

$$S_N = C_{NS}/a_N \tag{4}$$

$$a_N = c_{NS}/c_{NS}^0 \tag{5}$$

$$C_{NS} = k_s C_W \hat{V}_W c_{NS} \tag{6}$$

$$k_s = \exp(-\beta_{NS}/C_W) \tag{7}$$

where C_{NS} denotes the concentration of dissolved solute in the polymer matrix when the latter is equilibrated with a bulk solution of concentration c_{NS}; c_{NS}^0 is the saturation value of c_{NS}; $\hat{V}_W$ is the specific volume of the solvent; and k_s is defined in such a way as to reduce to unity if the solute is sorbed merely by dissolution in the imbibed solvent and the solvating power of the latter is equal to that of the bulk solvent. Thus, for a system of the type considered here (with water as the solvent, a simple electrolyte as the solute, and an effectively uncharged polymer), k_s would be expected to approach unity in strongly hydrophilic polymer matrices. This behavior is well represented by eq. (7) in which β_{NS} is a constant, the value of which determines the steepness of the variation of k_s as the hydrophilicity of a particular kind of polymeric material is varied. Note that, as shown by eqs. (4)–(6), S_N represents, in effect, the saturation value of C_{NS} at a given C_W. As in Petropoulos et al.,[3] we set $S_N(C_W^0) = C_{NS}^0$.

The diffusion of the solvent is described by

$$D_W = D_{WO}\exp(\beta_W C_W) \tag{8}$$

where $D_{WO} = D_W(C_W = 0)$ and β_W allows for the dependence of D_W on the concentration of imbibed solvent.

The rate of diffusion of (dissolved) solute is strongly affected by the extent to which the polymer is swollen by the solvent. A mathematically

convenient two-parameter representation of this effect, adopted in Petropoulos et al.,[3] on the basis of the "free volume theory" of Yasuda and colleagues,[4,5] is

$$D_N = D_{NS}\exp[-\beta_{N1}/(\beta_{N2} + C_W)] \qquad (9)$$

where D_{NS} is the diffusion coefficient in the bulk solvent, β_{N1} and β_{N2} are (adjustable) constants, and $\beta_{N2} = 0$ or $\beta_{N2} > 0$ in the simpler or more elaborate versions of the aforementioned theory, respectively. It is noteworthy that this theory was successfully applied to polymer-soluble drug systems.[6,7]

On the basis of eqs. (3)–(9), eqs. (1) and (2) were solved simultaneously in Petropoulos et al.[3] by an explicit finite difference method that uses a polymer-fixed frame of reference[8a] and boundary conditions representative of solute release kinetic experiments as follows[3]:

$$a_W = a_{WO};\ a_N = a_{NO};\ C_W = C_{WO};$$
$$C_N = C_{NO} \text{ at } t = 0,\ 0 < x \le l \qquad (10a)$$
$$a_W = 1;\ a_N = 0;\ C_N = 0 \text{ at } t \ge 0,\ x = 0 \qquad (10b)$$
$$\partial a_W/\partial x = \partial a_N/\partial x = 0 \text{ at } t \ge 0,\ x = l \qquad (10c)$$

where $x = l$ at the midplane of the film and $x = 0$ at the surface exposed to the bulk solvent.

Note that under the aforementioned conditions 1 and 2, the above instantaneously reversible homogeneous osmotic swelling model (IRHOSM) duly reduces to normal Fickian[8b] or Higuchi[2] kinetics, namely (for $M_{Nt}/M_{N\infty}$ sufficiently low to preserve the condition $C_N \cong C_{NO}$ at $x = l$),

$$M_{Nt}/M_{N\infty} = 2[D_N t/\pi l^2]^{1/2} \qquad (11)$$

or

$$M_{Nt}/M_{N\infty} = [2D_N C^0_{NS} t/l^2 C_{NO}]^{1/2} \qquad (12)$$
$$= (2P_N c^0_{NS} t/l^2 C_{NO})^{1/2}$$

according to whether $C^0_{NS} \cong C_{NO}$ or $C^0_{NS} \ll C_{NO}$, respectively. In eqs. (11) and (12) M_{Nt} and $M_{N\infty}$ represent the amount of solute released at times t and $t \to \infty$, respectively; $P_N = KD_N$ is the permeability of the solute; and K is the partition coefficient (assumed constant) as defined in part I.[1]

In practice the assumption of instantaneously reversible swelling is liable to break down in the case of stiff chain polymeric matrices due to the relatively slow rate at which the requisite polymer chain rearrangements can occur in the swelling (deswelling) matrix. This leads to non-Fickian solvent absorption (desorption) kinetics (i.e., sorption kinetics partly controlled by polymer chain relaxation processes)[9,10] and possibly solvent absorption–desorption hysteresis.[9]

Furthermore, solute dispersions are, in practice, frequently too coarse to conform to the model assumption of homogeneous polymer swelling.

Note, however, that sparingly soluble, osmotically inactive solute particles dispersed in a matrix consisting of flexible polymer chains, which tend to collapse around the particles as the latter are being dissolved away by imbibed solvent, will give rise to a situation in close conformity to that envisaged in the model. If the solute particles are too large or the polymer chains too stiff, the eluted particles will leave behind microscopic gaps, which will fill with solvent as seen in part I.[1] From the analysis of release kinetics viewpoint, however, this deviation from the IRHOS model assumptions (which require the transport properties of the matrix to revert to those of the neat polymer upon solute depletion) is not serious, because the low solubility of the solute ensures $C^0_{NS} \ll C_{NO}$. Under these conditions the profile of the solute concentration across the film takes the form of a sharp front separating an inner fully loaded from an outer fully particle-depleted region, and the release process is rate controlled by transport of (dissolved) solute across the latter region, in conformity with eq. (12) (see, e.g., full line C in fig. 5 of Petropoulos et al.,[3] which, incidentally, should have been labeled D, while the full line D of that figure should have been labeled C). Thus, P_N in eq. (12) may be unambiguously assigned the value characteristic of the fully particle-depleted matrix as in part I.[1] The only complication that might be plausible would be a tendency of the polymer chains surrounding the solvent filled cavities or globules of the solvent to collapse (or otherwise relax) slowly during the course of the release process, thus causing P_N to vary with time. The data of part I showed no evidence of any such behavior.[1]

Hence, material deviations from the model assumptions are to be expected mainly in the case of sizeable, soluble, osmotically active solute particles. A widely accepted[11–16] nonhomogeneous osmotic swelling mechanism of solute release may be summarized as follows: incoming solvent contacts an encapsulated solute particle, a saturated solution of solute is formed within the relevant cavity or "capsule," the latter swells as more sol-

vent is osmotically driven in, and the cavity wall finally cracks or ruptures under the mechanical stress. Therefore, this "cavity-wall rupture" (CWR) mechanism tends to generate permanent passageways between neighboring cavities, thus helping to create continuous liquid solvent pathways through interlinked solvent filled cavities (globules) in the particle-depleted matrix, which can greatly enhance the rate of solute release by comparison with that from fully encapsulated particles.[1]

Reliable prediction of the operation of a CWR mechanism in a particular practical situation is very difficult. However, because the relevant morphological changes of the polymeric matrix are obviously irreversible, occurrence of a CWR mechanism can be experimentally demonstrated by studying the transport properties of the solute-depleted matrix in comparison with those of both the neat polymer and a similar matrix depleted of an osmotically inactive solute.

For this purpose, detailed measurements of solvent and solute sorption and diffusion in both particle-depleted and neat polymer matrices were performed. To ensure comparability with the data on osmotically inactive solutes acquired in Part I,[1] cellulose acetate (CA) of the same composition and identical film-forming procedures were employed here, using NaCl (of particle size similar to that of the $CaSO_4$ utilized in Part I[1]) as the osmotically active particulate solute. Finally, the pattern of solute release behavior to be expected for the IRHOS was established as a basis for comparison with the observed release behavior through model calculations using eqs. (1)–(10) in conjunction with the measured solute transport properties of the neat matrix.

The results obtained by the above methods provided conclusive evidence against a CWR mechanism of release and led us to propose a more general nonhomogeneous osmotic swelling model, which includes the CWR mechanism as a special case.

The notation of part I of this study[1] is preserved here as much as possible.

EXPERIMENTAL

Preparation of NaCl Particle-Loaded Polymer Matrices

Thin films of CA (of thickness $2l$ = 170–340 μm) containing various amounts of NaCl were prepared by the same method and from CA of the same composition (Eastman Chemicals, Switzerland; type CA-398-30; acetyl content 39.8 wt %) as in part I.[1] The polymer was dissolved (up to 20 wt %) in a stirred dispersion of the appropriate amount of salt powder in acetone and cast on a glass plate followed by slow evaporation of the solvent. NaCl particles (3–10 μm) were obtained by addition of acetone or alcohol to stirred saturated aqueous salt solutions. The dried precipitate was ground in a mortar and passed through a fine sieve to eliminate any relatively large particulate aggregates as far as possible.

Particulate Salt Release Experiments

The release experiments were performed by mounting the (ca. 3×3 cm^2) salt-containing polymer film specimen [initially conditioned at 40% relative humidity (RH)] on a stirring rod rotating at a rate of 250–300 rpm in a known volume of CO_2-free distilled water that was thermostatted at 25°C and renewed at frequent intervals. The amount of salt released M_{Nt} as a function of time was monitored by measuring the ionic conductivity of the desorbing bath using a YSI (model 31) conductivity bridge. The results were often checked by atomic absorption assay of sodium in a Perkin–Elmer 2380 atomic absorption spectrophotometer. In selected cases, the concurrent variation of the water content of the film was also monitored by briefly interrupting the release experiment at appropriate intervals and weighing the carefully blotted film. The water content of the film was estimated each time after allowing for the weight lost due to the desorption of salt.

Determination of Partition and Diffusion Coefficients of NaCl

Particle-Depleted Films

At the end of selected particulate salt release experiments, the resulting fully salt-depleted film specimens were equilibrated with 0.05 g cm^{-3} aqueous NaCl solutions at 25°C to determine the partition coefficient K of NaCl therein, defined as $K = C_{NS}$ (g cm^{-3} of hydrated matrix)/c_{NS} (g cm^{-3} of solution). Care was taken to ensure that equilibration times were well above those required [according to the long time counterpart of eq. (11) analogous to eq. (11b) given below][8b] to attain 99% of the final equilibrium value.

After equilibration, the films were immersed

for 1 s in water (to remove solution adhering to the film surfaces), blotted, and subjected to release tests at 25°C as described in the preceding section to determine the diffusion coefficient of NaCl therein. The water content of the film before and after the release test was estimated gravimetrically.

Neat Films

Similar sorption equilibrium and desorption kinetic experiments were also performed with neat films; these films were prepared as above but without the addition of salt to the dope before casting, hence being free of inhomogeneities due to microscopic gaps left behind by the eluted salt particles.

Determination of Water Uptake

The rate of water absorption by particle-depleted or neat films was measured by immersion in water, followed by blotting and weighing in a weighing bottle at various times. The film specimens were previously either dried by evacuation or conditioned to a low RH. To determine the final amount of water absorbed as precisely as possible, the film was weighed several times during the following few days.

RESULTS

Kinetic Behavior of Particulate Salt-Loaded Films

Typical results of NaCl release kinetics from films of two different thicknesses and three different particulate salt loads are presented in Figures 1 and 2, respectively. As illustrated in both figures, good reproducibility was found between samples taken from the same film, as well as between samples from different films containing the same salt load. Figure 1 also demonstrates that the kinetics of release was not significantly dependent on film thickness.

Lines N1–N3 in Figure 2 show that salt load had a substantial effect on particulate salt release kinetics. In particular, at the highest salt load, the release curve plotted on a $\sqrt{t}$ scale is linear (as was the rule in the case of sparingly soluble salts[1]) but becomes progressively more S shaped (i.e., exhibits a progressively more prominent "acceleration effect" in the middle $M_{Nt}/M_{N\infty}$ range) at lower salt loads. The corresponding fractional

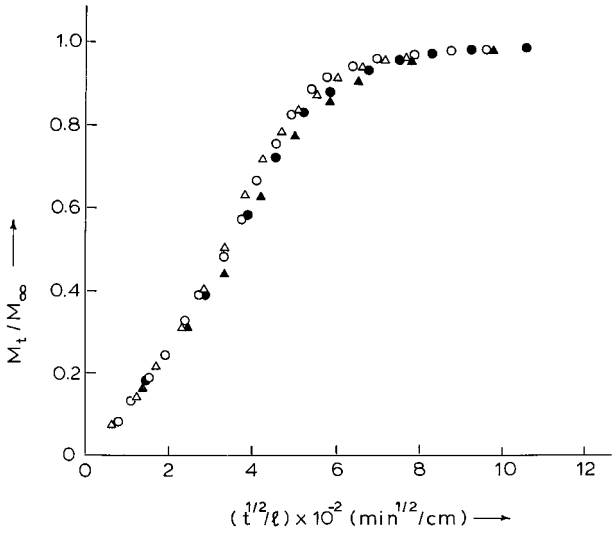

Figure 1 NaCl release from cellulose acetate films of various thicknesses, containing 11.1 wt % of particulate salt (fractional volume, $\varepsilon_N = 0.061$). The hydrated film thickness (at the end of the experiment) was (●, ▲) 170, (○) 250, and (△) 330 μm.

release rates do not vary substantially with the salt load (especially at short times) in contradistinction to what was observed in the case of sparingly soluble salts (see figs. 1, 2 of Part I[1]). It is noteworthy that (as is usually the case with osmotically active solutes) these particulate fractional release rates are much higher than that of salt dissolved in the neat polymer matrix (represented by line N in Fig. 2). The latter conforms to eq. (11) in the linear M_{Nt} versus $\sqrt{t}$ range (see below) and is, therefore, independent of salt load (as long as the variation of salt load does not give rise to significant changes in C_W).

Figures 2 and 3 show examples (see lines W1 and W2 therein) of measurements of the concurrent evolution of the water content of the solid matrix (starting with a salt-loaded matrix conditioned at RH $\sim$ 0.4) comprising (1) water hydrating the neat polymer; (2) water filling microscopic cavities left behind by the eluted particles (v.s.) or any gaps that had been left in the original solid matrix (due to failure of the polymer to penetrate narrow interstices between particles in close contact at the preparation stage), as in the case of sparingly soluble salts[1]; plus (3) excess water temporarily retained in the matrix as a result of the osmotic action of the solute, which is, of course, releasable upon salt depletion.

Water sorbed under the latter condition is thus responsible for the fact that the total measured

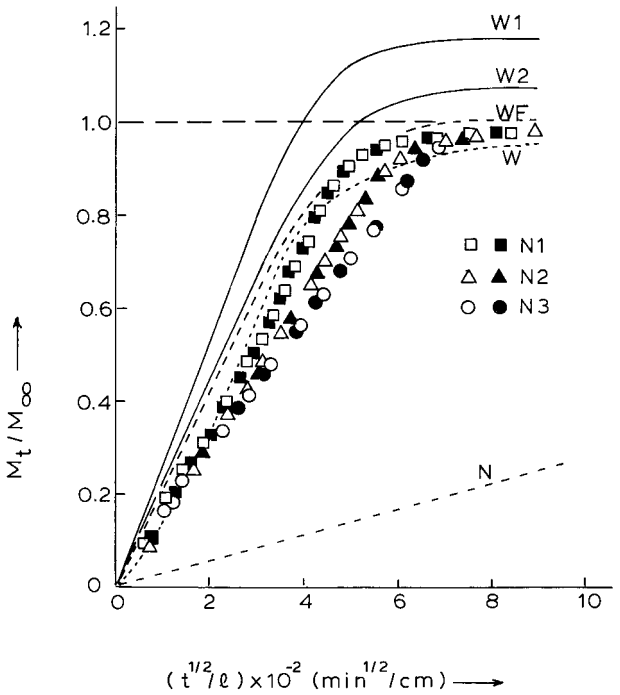

Figure 2 Release of NaCl from duplicate samples of cellulose acetate loaded with NaCl particles and containing a fractional volume of salt, ε_N of 0.061 (line N1), 0.115 (N2), or 0.223 (N3). The hydrated film thickness was ca. 300 μm. The concurrent measured water uptake corresponding to lines N1 and N2 is represented by lines W1 and W2, respectively. Water absorption by a neat cellulose acetate film (line W) and dissolved NaCl release from a neat film previously equilibrated with a 0.05 g cm^{-3} NaCl solution (line N) are shown for comparison. The theoretical line WF represents Fickian water absorption with $D_W = 6 \times 10^{-8}$ cm^2 s^{-1}.

water uptake during salt release can exceed the final equilibrium water content of the salt-depleted film,[17–21] an effect that is particularly noticeable in Figures 2 and 3 at the lowest salt load (line W1). However, as illustrated in these figures, loss of this temporarily sorbed water is here a slow process, which continues long after salt release is complete. Undoubtedly, this is attributable to the same slow macromolecular relaxation effects responsible for the correspondingly slow approach to equilibrium observed during the uptake of liquid water (or water vapor at high RH[9]) by neat CA film, as illustrated by line W in Figures 2 and 3. This slow approach to equilibrium can be better appreciated by comparing line W with the theoretical Fickian curve shown in Figure 2 (see line WF therein) that was calculated on the basis of

$$M_{Wt}/M_{W\infty} = 2(D_W t/\pi l^2)^{1/2} \quad \text{at} \quad M_{Wt}/M_{W\infty} \leq 0.5 \quad (11a)$$

and

$$M_{Wt}/M_{W\infty} = 1 - (8/\pi^2)\exp(-D_W \pi^2 t/4l^2) \quad \text{at} \quad M_{Wt}/M_{W\infty} > 0.5 \quad (11b)$$

with $D_W = 6 \times 10^{-8}$ cm^2 s^{-1}. For completeness, one may note that (as in the case of sorption from the vapor phase[9]) the experimental absorption curve W tends to be S shaped, indicating the presence of a second relatively fast macromolecular relaxation process,[9] which is of no immediate concern to us here. A more noteworthy point in the present context is the generally small difference in the fractional rate of water uptake between particulate salt-loaded and neat films shown in Figure 2; this contrasts with the large difference in salt release rate noted above between films loaded with particulate salt and neat films containing dissolved salt, respectively.

Equilibrium Uptake of Water and NaCl by Neat and Particle-Depleted Films

Replicate measurements of equilibrium uptake of water and NaCl by neat and particle-depleted film samples were performed and the results obtained are summarized in Tables I and II. The latter samples were derived from films originally loaded with salt particles up to a fractional volume, ε_N, of 0.1 to preserve, as far as possible, conditions justifying (on the basis of the findings of Part I[1]) the assumption that the salt particles were fully enveloped by polymer without leaving air gaps in the solid matrix. The observed water regain C_W^0 and salt partition coefficient K for neat films agree reasonably well with those reported by other workers.[22,23] Some variability of the measured values of C_W^0 and K (attributable to variability of polymer microstructure[24]) was found (as illustrated in Tables I, II), the latter being in part a consequence of the former with the result that the corresponding values of k_s tended to be significantly less variable. However, in keeping with theoretical expectation (see above and Petropoulos et al.[3]), k_s also tended to increase with increasing C_W^0.

It is of particular interest to repeat here the comparison made in part I[1] between the observed fractional volume of imbibed water (ε_W) in the particle-depleted films and the sum of the (calcu-

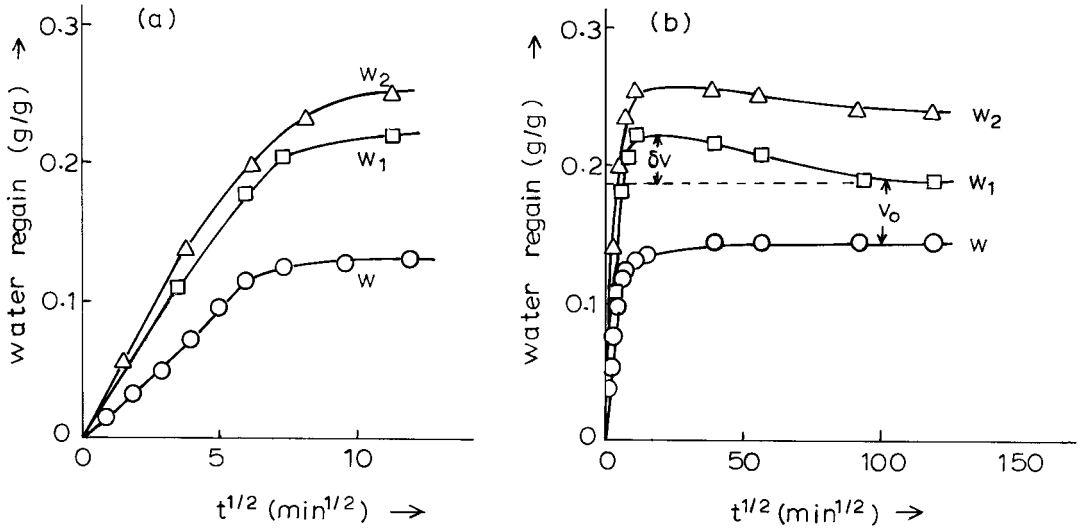

Figure 3 Lines W, W1, and W2 of Figure 2 replotted on (a) short or (b) long time scales to show the evolution of the absolute water content of the film (in grams per gram of dry polymer) during and after the salt release experiment. V_0, amount of water replacing salt particles; δV, maximum amount of osmotically imbibed water.

lated) fractional volumes of water and salt ($\varepsilon_{WP} + \varepsilon_N$) in the corresponding original salt-loaded films, assuming the polymer therein to be fully hydrated and the complete absence of air gaps (v.s.). Table I shows that $\varepsilon_{WP} + \varepsilon_N \cong \varepsilon_W$ within experimental error; this indicates that, as was found in part I,[1] the loss in volume due to salt elution is compensated by the additional irreversible uptake of an equivalent volume of water.

In the case of the sparingly soluble, osmotically inactive salts studied in part I,[1] the additional imbibed water could be reasonably considered to be in the form of globules replacing the original salt particles; this interpretation is confirmed by the fact that, for the low solute loads of interest here, the permeability P_N of the salt-depleted matrix was enhanced by the presence of this additional imbibed water only marginally above that of the neat polymer P_{NM}. If the same interpretation was applicable in the present context, it would mean that the excess swelling induced by the osmotically active salt load does not produce any irreversible morphological changes in the polymer matrix. A useful check of this important point is afforded by the measured values of k_s for the particle-depleted films. Water globules as large as the NaCl particles used should undoubtedly be characterized by $k_s = 1$; hence, denoting by k_{s1} the expected value of k_s for the particle-depleted film, if the above interpretation is valid, we have

$$k_{s1} = k_s^0 \varepsilon_{WP}/\varepsilon_{WO} + (1 - \varepsilon_{WP}/\varepsilon_{WO}) \quad (13)$$

where ε_{WO} is the fractional volume of water imbibed by the salt-depleted film under the conditions of the partition coefficient measurement (c_{NS}

Table I Observed Equilibrium Water Regain (C_W^o, g g^{-1} Dry Polymer) and Corresponding Volume Fraction of Imbibed Water (ε_W) in Particle-Depleted Films (Calc Vol Fraction Occupied by Original Particles, $\varepsilon_N > 0$) or Neat Films ($\varepsilon_N = 0$, $\varepsilon_W = \varepsilon_{WP}$), demonstrating $\varepsilon_N + \varepsilon_{WP} \cong \varepsilon_W$

ε_N	C_W^o (g g^{-1})	ε_{WP}	$\varepsilon_N + \varepsilon_{WP}$	ε_W
0	0.145–0.155	0.164–0.174		
0.061	0.198–0.217	0.154–0.163	0.215–0.224	0.212–0.228
0.115	0.262–0.273	0.145–0.154	0.260–0.269	0.262–0.270

See the text.

Table II Sorption Equilibrium and Kinetic Parameters for Particle-Depleted ($\varepsilon_N > 0$) or Neat ($\varepsilon_N = 0$) Cellulose Acetate Films

ε_N	K	k_s	C_{WO} (g g^{-1})	C_W^0 (g g^{-1})	$D_N \times 10^9$ (cm^2 s^{-1})
0	0.0375	0.225	0.144	0.150	1.2
	0.0392	0.240	0.147	0.153	1.2
	0.0357	0.224	0.139	0.145	1.0
0.061	0.0683	0.337	0.184	0.198	4.4
	0.0758	0.361	0.192	0.206	3.7
	0.0910	0.410	0.206	0.217	6.4
	0.0677	0.335	0.184	0.200	2.9
0.115	0.131	0.510	0.248	0.273	8.3
	0.127	0.505	0.243	0.262	7.5

= 0.05 g cm^{-3}; see the Experimental section), which, strictly speaking, should be slightly less than ε_W; and k_s^0 is the measured value of k_s for the neat film. Table III shows that the calculated k_{s1} values significantly exceed the observed ones and are thus indicative of morphological changes induced by osmotic swelling, which result in a more homogeneous distribution of the additional water permanently taken up by the salt-depleted film than in the case of osmotically inactive solutes.[1]

On the other hand, a reasonable picture of the variation of k_s with ε_W or C_W under conditions of effectively homogeneous swelling may be obtained from measurements of k_s in CA materials of higher and lower acetyl content (and hence a lower or higher degree of hydration, respectively) than the material of interest here. Figure 4 shows that data of this kind reported by Lonsdale et al.[23] conform reasonably well to eq. (7) with β_{NS} = 0.207 g g^{-1}. Table III shows that the experimental k_s values tend to be higher than those (denoted by k_{s2}) predicted by the aforementioned correlation. [Fig. 4 correspondingly shows (cf. the broken line therein) that the relevant points tend to deviate increasingly from the correlation line with rising C_W.] These results are, therefore, consistent with the presence of water globules that are on average smaller in size than the salt particles they have replaced, the rest of the additional imbibed water being more homogeneously distributed in the matrix.

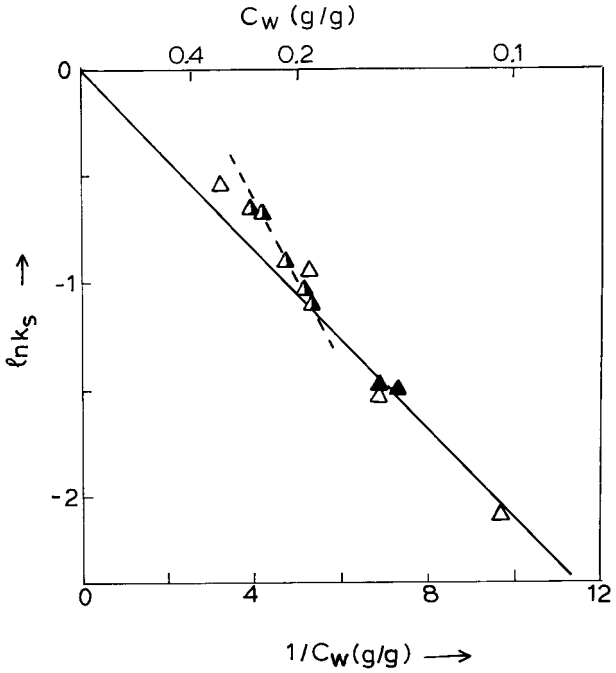

Figure 4 Dependence of k_s on degree of hydration (C_W in grams per gram of dry polymer) according to eq. (7) (full line corresponding to β_{NS} = 0.207 g g^{-1}) for (△) cellulose acetates of varying acetyl content[23] in comparison with experimental data from the present work for (▲) neat or (◮) particle-depleted films. The trend of the particle-depleted film data is indicated by the broken line.

Diffusion of NaCl and Water in Neat and Particle-Depleted Films

The diffusion behavior of water and NaCl in neat and particle-depleted films was studied by means

Table III Comparison of Experimental k_s Values with k_{s1} or k_{s2}

ε_N	C_{WO} (g g^{-1})	k_s	k_{s1}	k_{s2}
0	0.139–0.147	0.22–0.24		
0.061	0.184–0.206	0.34–0.41	0.44–0.46	0.32–0.36
0.115	0.243–0.248	0.50–0.51	0.55–0.57	0.42–0.43

k_{s1} and k_{s2} were calculated on the basis of eq. (13) or eq. (7) (with β_{NS} = 0.207 g g^{-1}), respectively.

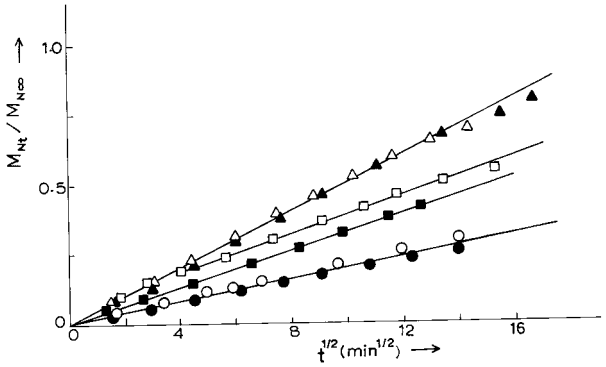

Figure 5 Release of dissolved NaCl ($C_{NO} < C^0_{NS}$) from (○, ●) neat or particle-depleted films with original salt content of ε_N = (□, ■) 0.061 or (△, ▲) 0.115. All film samples had been equilibrated previously with a NaCl solution containing 0.05 g cm^{-3}. The hydrated film thickness was ca. 300 μm.

of absorption (water) or desorption (NaCl) kinetic experiments as described in the Experimental section.

Some representative examples of NaCl desorption kinetics are shown in Figure 5. The initial portions of these curves were found to be linear on the $\sqrt{t}$ scale and to pass through the origin (provided that due care had been taken to eliminate surface salt prior to the commencement of the desorption experiment) in conformity with Fickian kinetics. The diffusion coefficient D_N was calculated in each case by means of eq. (11), where l refers to the half-thickness of the hydrated film. The resulting D_N values shown in Table II exhibit greater variability than the corresponding partition coefficients, as would be expected in view of the fact that diffusion properties generally tend to be more sensitive than sorption properties to variations in polymer microstructure. Nevertheless, there is an obvious tendency of D_N to substantially increase with the original salt load and hence with the total water content of the particle-depleted membrane. The resulting increase in permeability $P_N = KD_N$ may be compared with theoretical predictions for the case where the whole additional volume of permanently imbibed water ε_N is in the form of globules, as shown in part I.[1] In particular, application of the appropriate forms of the Maxwell and Böttcher equations, namely,[1]

$$\frac{P_N}{P_{NS}} = \frac{(1 + 2\varepsilon_N)P_{NM}}{(1 - \varepsilon_N)P_{NS}} \qquad (14)$$

$$\frac{P_N}{P_{NS}} = \frac{P_{NM}}{(1 - 3\varepsilon_N)P_{NS}} \qquad (15)$$

(where P_{NS} and P_{NM} are the permeabilities of salt in water and in neat hydrated polymer, respectively) yields the results shown in Table IV. The experimental P_N values are ca. 1 order of magnitude higher than the calculated ones, confirming our previous conclusion that the additional water imbibed by salt-depleted films is more homogeneously distributed in the polymer than would be the case if the said additional water merely replaced the eluted salt particles.

On the other hand, a useful picture of the dependence of D_N on the degree of hydration under conditions of effectively homogeneous swelling is afforded by Figure 6. This figure shows that eq. (9) with β_{N1} = 1.92 g g^{-1} and β_{N2} = 0.05 g g^{-1} provides a reasonably good representation of the functional dependence of D_N on C^0_W for the series of CA materials referred to above in connection with Figure 4. The fact that the experimental point for the more highly particle-depleted film in Figure 6 falls significantly below the correlation line is also in keeping with our previous conclusion that the aforesaid additional imbibed water is not as uniformly distributed as the normal water of hydration of the polymer.

The non-Fickian water uptake kinetic behavior of the neat film was discussed above (the relevant curve in Fig. 7 is identical with line W in Fig. 2). Figure 7 shows that the fast molecular relaxation process detected in the neat film was wiped out in the particle-depleted film, while the slow relaxation responsible for the slow approach to equilibrium became more prominent. However, there was not much difference in the rate of uptake over most of the $M_{Wt}/M_{W\infty}$ range.

DISCUSSION AND CONCLUSIONS

Deviations from Fickian Kinetic Behavior

Both complications of the observed kinetic behavior of particulate NaCl-loaded films reported above, namely the deviation from $\sqrt{t}$ solute release kinetics (in the form of an "acceleration effect" resulting in an S-shaped M_{Nt} vs. $\sqrt{t}$ release curve) and the temporary retention of excess imbibed water, were previously observed in other systems[15–21] and were successfully reproduced[3] by calculations based on the IRHOS model of eqs.

Table IV Experimental NaCl Permeabilities of Neat ($\varepsilon_N = 0$, $P_N = P_{NM}$) and Particle-Depleted ($\varepsilon_N > 0$) Films and Comparison of Exptl P_N/P_{NS} Values for $\varepsilon_N > 0$ with Those Predicted from Eqs. (14) or (15) Using $P_{NM}/P_{NS} = 2.8 \times 10^{-6}$

ε_N	Exptl P_N ($cm^2\ s^{-1}$)	P_N/P_{NS} Exptl	Eq. (14)	Eq. (15)
0	4.2×10^{-11}	2.8×10^{-6}		
0.061	3.5×10^{-10}	2.3×10^{-5}	3.4×10^{-6}	3.5×10^{-6}
0.115	1.0×10^{-9}	6.7×10^{-5}	3.9×10^{-6}	4.3×10^{-6}

(1)–(10). (The former effect is also predictable on the basis of another more simplified model of this type.[25])

As far as the first effect is concerned, the relevant model calculations of Petropoulos et al.[3] indicate that it may be expected under conditions where solute transport is strongly affected by the degree of swelling of the polymer matrix and solvent uptake is not much faster than solute release (see fig. 2 of Petropoulos et al.[3]), and it is intensified in the presence of osmotic swelling (see fig. 6 of Petropoulos et al.[3]). Reference to Figure 2 shows that the most pronounced observed solute release acceleration effect does indeed correlate with the most intense observed reversible osmotic swelling. So, the theoretical interpretations provided by the aforesaid model are useful in this particular respect and at the qualitative level.

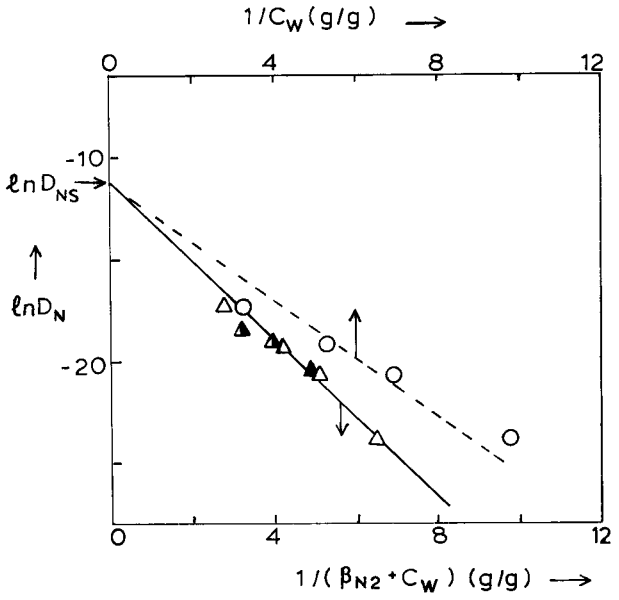

Figure 6 Dependence of D_N on degree of hydration for cellulose acetates of varying (○, △) acetyl content[23] correlated by means of the (---, ○) simple or (—, △) more elaborate versions of the free volume theory represented by eq. (9). A satisfactory correlation is obtained in the latter case for $\beta_{N2} = 0.05$ g g^{-1} ($\beta_{N1} = 1.92$ g g^{-1}), and our experimental data for (▲) neat and (◮) particle-depleted films are compared with this correlation.

Calculated Behavior for IRHOS

At the quantitative or semiquantitative level, the IRHOSM can provide a useful basis for comparison of the kinetic behavior actually observed against what could typically be expected under conditions of fully and instantaneously reversible homogeneous osmotic swelling (leading to Fickian water absorption–desorption by the polymer). To this end, model computations were performed that were analogous to those of Petropoulos et al.[3] but embodied, as far as possible, the salient features of the system under consideration on the basis of the experimental information reported

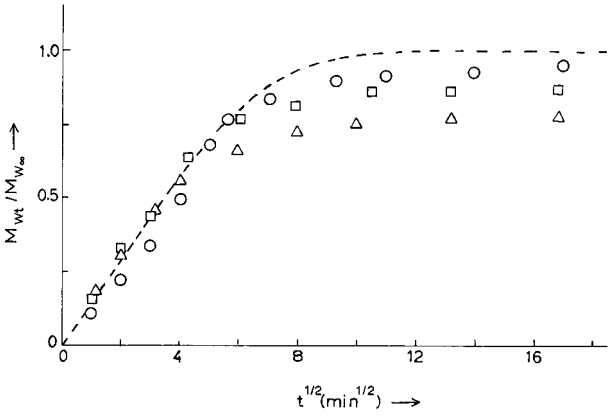

Figure 7 Absorption of water by (○) neat or particle-depleted [original salt content, ε_N = (□) 0.061 or (△) 0.115] films previously dried by evacuation. The film thickness was ≅ 300 μm. The line represents Fickian diffusion for $D_W = 6 \times 10^{-8}$ $cm^2\ s^{-1}$ and $2l = 300$ μm.

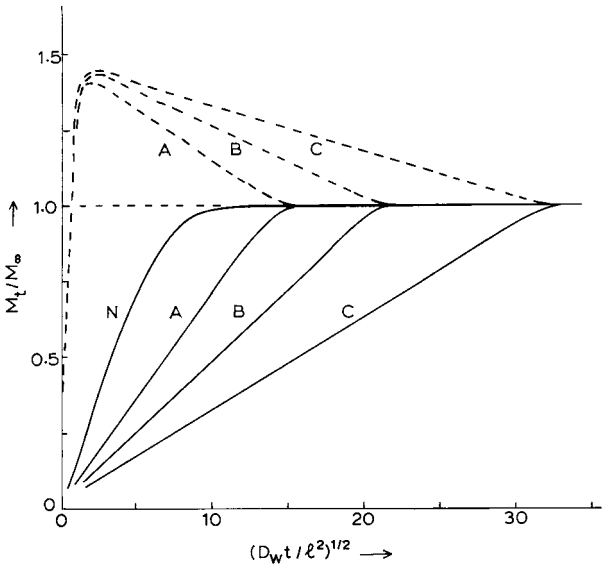

Figure 8 Model computations [on the basis of the IRHOSM of eqs. (1)–(10)] of (---) water uptake and (—) salt release kinetic curves for $f_{NS} = C^0_{NS}/C_{NO} = 0.108$ (curve A), 0.054 (curve B), and 0.025 (curve C); $K_{W3}C_{NO} = 0.5$. For other parameters see text. The dissolved salt release curve (line N) is also shown for comparison.

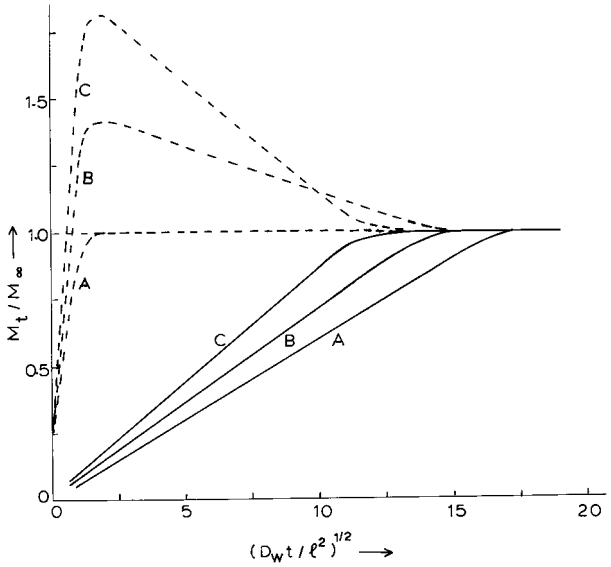

Figure 9 IRHOSM (---) water uptake and (—) salt release kinetic curves for $C^0_{NS}/C_{NO} = 0.108$; $K_{W3} = 0$ (curve A) or $K_{W3}C_{NO} = 0.5$ (curve B) or 1.0 (curve C). For other parameters see text.

above. The values of β_{NS}, β_{N1}, and β_{N2} resulting from Figures 4 and 6 were used in conjunction with $D_{NS} = 1.5 \times 10^{-5}$ cm^2 s^{-1} for NaCl in aqueous solution. A value of $D_W = 6 \times 10^{-8}$ cm^2 s^{-1}, corresponding to line W of Figure 2 (with $\beta_W = 0$ for simplicity[3]), appeared to be the most appropriate choice for the present purposes in conjunction with $a_{WO} = 0.4$ (representing the RH to which the salt-loaded film samples were typically exposed prior to the release experiments), which for neat film yields $C_{WO} = 0.25_6 C^0_W$ on the basis of $K_{W1} = 0.4\ C^0_W$ and $K_{W2} = 0.6\ C^0_W$ previously used[3] and adopted here too, and with $C^0_W = 0.15$ g g^{-1} taken from Table I. Calculations were performed for $f_{NS} = C^0_{NS}/C_{NO} = 0.108$, 0.054, or 0.025 (which correspond to the experimental ε_N values of 0.061, 0.115, or 0.223, respectively) in the absence ($K_{W3} = 0$) or presence ($K_{W3}C_{NO} = 0.5$ or 1) of solute osmotic action.

The resulting computed model salt release and corresponding water uptake kinetic curves are given in Figures 8 and 9, and examples of the computed salt and imbibed water profiles across the film are shown in Figure 10.

Rates of water uptake are generally well reproduced, not surprisingly in view of the observed general insensitivity of these rates to experimental conditions (cf. line WF with W1, W2 in Fig. 2). The experimental water sorption data differ from the model results by (1) the presence of additional permanently imbibed water in the salt-depleted film, (2) the delayed loss of excess water temporarily taken up as a result of solute osmotic action, and (3) the diminishing amount of such temporarily imbibed water with increasing salt load. The first two differences are as expected, in

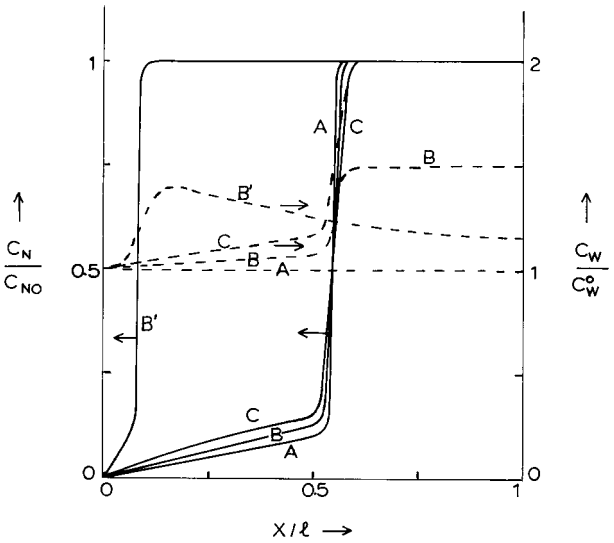

Figure 10 Computed (---) water and (—) salt diffusion profiles corresponding to the kinetic curves of Figure 9 at $M_{Nt}/M_{N\infty} = 0.5$ (curves A–C) or 0.09 (curve B′).

Table V Effective Salt Permeabilities Obtained from Results of IRHOSM Computations by Application of Eq. (12)

		P_N (cm^2 s^{-1})		
ε_N	C^o_{NS}/C_{NO}	$K_{W3} = 0$	$K_{W3}C_{NO} = 0.5$	$K_{W3}C_{NO} = 1.0$
0.061	0.108	4.0×10^{-11}	5.6×10^{-11}	8.0×10^{-11}
0.115	0.054	4.0×10^{-11}	5.3×10^{-11}	6.1×10^{-11}
0.223	0.025	4.0×10^{-11}	4.9×10^{-11}	5.4×10^{-11}

See Figures 8 and 9 for the results of the computations.

view of the particulate nature of the solute and the slow molecular relaxation of the polymer (v.s.); the third remains unexplained (v.i.).

On the other hand, the computed fractional salt release rates for $C^0_{NS}/C_{NO} < 1$ do not differ widely from that of the dissolved salt, which, as was seen above (cf. Fig. 2), is much lower than the observed release rates of particulate salt. Solvent uptake is thus too fast by comparison with the computed rate of salt release to give rise to any sizeable deviation of the latter from $\sqrt{t}$ kinetics.

Figure 9 shows further that in the presence of degrees of solute osmotic activity giving rise to reversible osmotic swelling of intensity comparable to or exceeding that observed experimentally (cf. Fig. 2), only relatively modest enhancement of the aforementioned computed salt release rates is achieved. This is not altogether surprising in view of the fact that in spite of the high water solubility of NaCl, the prevailing kinetic conditions (notably the condition $C^0_{NS} \ll C_{NO}$) do not differ materially from those for sparingly soluble salts discussed in the Introduction: here too reasonably sharply separated, fully loaded and fully disperse solute depleted regions develop (see Fig. 10), resulting in release kinetics conforming to eq. (12) with P_N characteristic of solute transport in the latter region (which, according to the model assumptions, is identical with the neat polymer). Accordingly, osmotic swelling, which is assumed in the model to be instantaneously reversible (v.s.) and is therefore confined to the solute-loaded region, can affect the rate of solute release only indirectly and only to a modest extent by giving rise to a steeper solute concentration profile in the depleted region, as illustrated in Figure 10.

Because the aforementioned computed release curves do not exhibit any significant deviation from $\sqrt{t}$ release kinetics, effective P_N values may be determined by application of eq. (12) (see Table V). The fact that in the absence of osmotic swelling these effective P_N values do not differ significantly from P_{NM} constitutes a useful check of the accuracy of the computations.

Comparison of Experimental with IRHOSM Permeabilities

Effective P_N values may be determined similarly from the particulate NaCl release data of Figure 2, at least in the case of the higher salt loads where the deviation from $\sqrt{t}$ kinetics is small or absent (see Table VI). They turn out to be higher than the corresponding IRHOSM computed ones by ca. 2 orders of magnitude.

For the highest NaCl load (which corresponds to a salt volume fraction $\varepsilon_N = 0.22$), this is as expected because much the same relative difference between P_N and P_{NM} was found at this ε_N value for particulate $CaSO_4$ release (see table IV of part I[1]). The latter result is correlated with incomplete coating of the embedded salt particles with polymer, indicated by the appearance of gaps in the $CaSO_4$-loaded matrix (detected through the corresponding increase of imbibed water), due to

Table VI Experimental Effective Permeabilities of NaCl (P_N) Derived from Particulate Salt Release Data (Fig. 2) by Application of Eq. (12)

C_{NO} (g cm^{-3})	ε_N	P_N (cm^2 s^{-1})
0.002	0	4.2×10^{-11}
0.133	0.061	(1.0×10^{-8})[a]
0.249	0.115	1.5×10^{-8}
0.483	0.223	2.1×10^{-8}

The corresponding value for the neat film ($\varepsilon_N = 0$, $P_N = P_{NM}$) is shown for comparison.

[a] Derived from the initial linear part of the relative curve.

the inability of the viscous polymer solution to penetrate narrow interstices between juxtaposed particles at the preparation stage.[1] This leads to the formation of continuous aqueous pathways in the particle-depleted matrix, consisting of strings of water globules (replacing the original salt particles) interconnected by the aforesaid gaps filled with water, which can greatly enhance P_N, as discussed in previous sections and in part I.[1]

On the other hand, P_N is enhanced relative to P_{NM} to much the same extent at the lower particulate NaCl loads ($\varepsilon_N = 0.11$ or $\varepsilon_N = 0.06$) while the P_N for $CaSO_4$ drops precipitously to a value only marginally above P_{NM} at $\varepsilon_N = 0.1$ (see table IV of part I[1]). The latter behavior is in keeping with salt particles completely coated with polymer (evidenced by the absence of gaps in the relevant original $CaSO_4$-loaded matrix), which are transformed into isolated water globules in the particle-depleted matrix (as indicated in the preceding section and in part I[1]). This leaves no room for doubt that the embedded NaCl particles are also fully enveloped by polymer, at least in the case of $\varepsilon_N = 0.06$. The observed enhancement of P_N relative to P_{NM} must therefore be attributed to the fact that water uptake in the particulate NaCl release is accompanied by morphological changes of the polymer matrix favoring the extensive creation of facile solute transport pathways. Clearly, these morphological changes are partly irreversible (and thus identifiable by suitable analysis of the transport properties of the relaxed swollen salt-depleted matrix as demonstrated above) and partly reversible, as evidenced by the fact that the effective P_N values for the relaxed salt-depleted matrix are roughly 1 order of magnitude lower than those found for particulate salt release (cf. Tables IV, VI). The enhancement of P_N by the latter effect largely persists for the duration of the NaCl experiment, thanks to the very slow deswelling process that follows reversible osmotic swelling as previously noted and illustrated in Figures 2 and 3. Furthermore, it is noteworthy (cf. lines W1 and W2 in Fig. 3) that the decrease of additional permanently imbibed water that accompanies reduction of salt load from $\varepsilon_N = 0.11$ to $\varepsilon_N = 0.06$ tends to be compensated by an increase in temporarily sorbed excess water, thus helping to maintain the enhancement of P_N/P_{NM} at much the same high level.

We are now left with the task of determining what kind of osmotic swelling mechanism can plausibly account for this salt release and accompanying water uptake kinetic behavior.

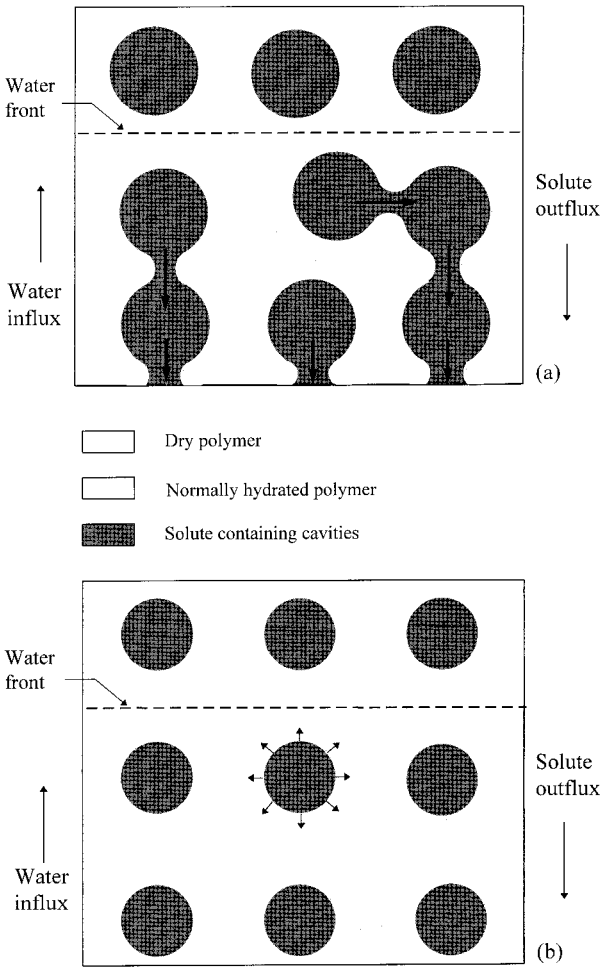

Figure 11 Idealized pictorial representation of the release of osmotically active solutes according to the CWR model (see text): (a) fast (➞) or (b) slow (→) release according to whether cavity wall rupture (giving rise to a system of interconnected cavities) can occur. [Fig. 11(b) was drawn on a scale representative of $\varepsilon_N = 0.06$.]

Applicability of CWR Model

An idealized pictorial representation of the predictions of the CWR model is given in Figure 11; it shows (following fig. 1 of Amsden et al.[15]) a sharp imbibed water front penetrating into successive layers of encapsulated water-soluble particles of solute. In each newly penetrated region, the polymer matrix is (presumably) hydrated to the normal extent characteristic of the neat polymer ($C_W = C_W^0$, see Introduction), while the particle-containing cavities also tend to dilate due to osmotically driven inflow of water. (The magnitude of the osmotic driving force varies directly with the solubility of the solute and the permse-

lectivity of the hydrated polymer matrix for solvent vs. solute, which, for the case under consideration, is $P_{WM}/P_{NM} = \varepsilon_W D_W/P_{NM} \approx 200$ and varies inversely with the degree of hydration.[23]) This tendency is resisted by the cavity walls that are thus subjected to increasing tangential tensile stresses while the limited dilatability of the cavities causes the hydrostatic pressure within them to rise. Accordingly, as previously pointed out, water flow into a particular cavity will continue until either the cavity wall undergoes (irreversible) mechanical failure [case A illustrated in Fig. 11(a)] or the aforementioned internal hydrostatic pressure rises to the point where the osmotic driving force is neutralized [case B illustrated in Fig. 11(b)].

According to the most common version of the CWR model,[15,16] mechanical failure in case A is visualized [see Fig. 11(a), which is simply a more idealized version of fig. 1 of Amsden et al.[15]] as a breach of the narrowest part of the cavity wall through which the aqueous solution formed by particle dissolution within the cavity can flow into the nearest neighboring cavity and ultimately to bulk solvent (via a network of such interlinked cavities extending through the preceding layers to the exposed surface of the matrix, as indicated in the Introduction). This picture obviously becomes increasingly unrealistic at lower solute loads, corresponding to thicker cavity walls.

This difficulty is circumvented by another version of the CWR model,[14] according to which mechanical failure occurs by the initiation of microcracks at the inner surface of the cavity walls; these microcracks then propagate in the matrix (at a rate dictated by the relevant tangential swelling stresses) until they run into neighboring cavities. Therefore, it appears that a CWR mechanism can, in principle, be invoked here down to the lowest salt load. The large difference between the value of P_N observed during particulate salt release and that characteristic of the (relaxed) particle-depleted matrix could then be attributed to partial "healing" of the microcracks (in a manner analogous to that observed in experiments of gas or vapor permeation through glassy polymer membranes[26,27]).

However, it is much more difficult to account for the large amount of excess water temporarily imbibed under these conditions, which, in the context of the CWR model, can only be regarded as representing dilation (δV) of particle-containing cavities before rupture. The original volume (V_0) of the latter is given, of course, by that of the solute particles at the beginning of the release experiment [or, equivalently, by the volume of excess imbibed water remaining in the relaxed salt-depleted matrix at the end of the release experiment; see Fig. 3(b)]. On this basis, a fractional cavity volume dilation of $\delta V/V_0 \approx 50\%$ is well within the range indicated by curve W1 of Figure 3. This implies that the cavity walls should be capable of sustaining a linear strain of $(\delta V/V_0)^{1/3} \approx 80\%$ without mechanical failure, which is well above the normal elongation at break for the CA matrices used here (table 4-13 in Lonsdale[28]).

Proposed More General Nonhomogeneous Osmotic Swelling Model

In the framework of the CWR model, case B [see Fig. 11(b)] can only give rise to solute release by "leakage" through the cavity walls and hence to release rates comparable with those observed for osmotically inactive solutes. According to the IR-HOSM, however, solute leakage out of a particle-containing cavity has the effect of enhancing the local degree of hydration of the surrounding matrix at the prevailing water activity to an extent determined by the local value of C_{NS}; this is, in turn, determined by the diffusion profile of leaking solute. One may thus expect [see eq. (3)] that, at sufficiently high prevailing water activity ($a_W \rightarrow 1$) and in the high C_{NS} region ($C_{NS} \rightarrow S_N$) adjoining the cavity, the normal maximum degree of hydration of the matrix C_W^0 may be substantially exceeded ($C_W = S_W a_W > C_W^0$). (Note, incidentally, that the swelling tangential tensile stresses referred to above, which are also most pronounced at the cavity–matrix interface, will also tend to enhance S_W, in accordance with the stress-dependent solubility coefficient model of Petropoulos[29,30]) Within these "zones of excess hydration" (ZEH) of the matrix adjoining the cavities, solute transport is, of course, facilitated and the permselectivity of the matrix is reduced, thus enhancing solute outflux from the cavity and abating the tendency of osmotically driven water influx thereto, respectively. Both these effects can be greatly intensified if the ZEH of neighboring particle-containing cavities (which gradually spread out as the leaking solute diffuses away from the cavity) overlap (as illustrated in Fig. 12) to an extent sufficient to create continuous pathways of facilitated solute transport extending to the exposed surface of the matrix at $x = 0$, in close analogy with the continuous aqueous pathways through strings of interlinked cavities

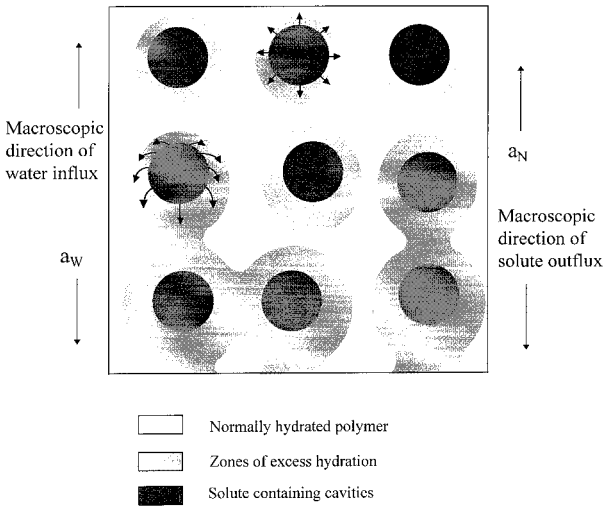

Figure 12 Idealized pictorial representation of the inhomogeneous osmotic swelling mechanism proposed here that involves zones of excess hydration wherein solute transport is facilitated. Thin arrows show the preferred microscopic transport direction of the solute. (This figure was drawn on a scale representative of $\varepsilon_N = 0.06$.)

shown in Figure 11(a). The main virtue of this new more general modeling approach is that mechanical failure of the polymer matrix remains a possibility but its occurrence is shown *not* to be a prerequisite for the observation of osmotically enhanced solute release.

Note that the pictorial representation of Figure 12 is not restricted by any assumption concerning the shape of the water penetration front. It is sufficient to specify a macroscopic decline of the penetrant water activity inward (upward in the figure) from $a_W = 1$ at the exposed surface, coupled with a macroscopic decline of solute activity a_N in the opposite direction to $a_N = 0$ at the exposed surface [see eq. (10)].

At any particular layer in the interior of the matrix, a_W will rise with the passage of time from a low initial value $a_W = a_{WO}$ to $a_W \to 1$ at the end of the experiment. This process will generally go through several stages.

Initially, as long as a_W is less than the critical value a_{W1} characteristic of the saturated aqueous solution of solute, water penetration into particle-containing cavities should not occur, except to the limited extent made possible by hydration of the particle surfaces. There follows a stage where $a_W \geq a_{W1}$ in the matrix, thus permitting osmotically driven water penetration into the aforementioned cavities, where a_W remains at $a_W = a_{W1}$ (imposed by the formation of a saturated aqueous salt solution therein[15]); initiation of ZEH as defined above is precluded because a_W still does not exceed the critical value a_{W2}, which would allow $C_W > C_W^0$. The latter value is given implicitly by the relation

$$a_{W2} S_W(a_W = a_{W2}, C_N = S_N) = C_W^0$$

Then, during a third stage (represented in the upper part of Fig. 12), where $a_W > a_{W2}$, ZEH can form and grow in intensity and extent as a_W rises and leaking solute diffuses outward from the cavities (as indicated by the thin arrows in the upper part of Fig. 12) down local microscopic solute activity gradients. (Because of the macroscopic water activity gradient, the growth of the ZEH is pictured in Figure 12 as being somewhat more pronounced in the $-x$ direction.)

Linkup (either direct or indirect, as illustrated in Fig. 12) with the ZEH formed in the preceding layer may be considered to mark the beginning of a fourth stage (represented in the middle part of Fig. 12). Here radial ZEH expansion is expected to slow down markedly because of the increasing tendency of leaking solute to follow the facile continuous pathways down the macroscopic solute activity gradient (i.e., downward in Fig. 12, as indicated by the thin arrows in the middle part of that figure). Consequently, the width of the ZEH that ultimately build up tends to be commensurate with the interparticle distance, thus accounting for the most prominent kinetic features discussed above: namely (1) the establishment of much the same continuous facile solute transport pathways in more and less concentrated fully encapsulated particle dispersions (represented by the cases of $\varepsilon_N = 0.11$ and $\varepsilon_N = 0.06$, respectively), and (2) the accompanying substantial rise in reversibly imbibed excess water (much of which can be accommodated in the ZEH) in the latter case.

This excess water is gradually lost during the final stage, which begins at the point where particulate solute within the relevant cavity is exhausted. Then, dissolved solute within the ZEH in excess of the local concentration imposed by the macroscopic solute activity gradient is, in turn, gradually lost, causing the ZEH to collapse accordingly (with ultimate expulsion of the water imbibed therein from the particle-depleted matrix), if the model assumption of full and instantaneous swelling reversibility is applicable. In the present system, the polymer chain relaxations that control the deswelling process are sufficiently slow to largely sustain the ZEH after local solute

depletion for the duration of the particulate NaCl release experiment (as illustrated in the lower part of Fig. 12).

The difference in morphology between NaCl and $CaSO_4$ particle-depleted matrices is also consistent with the proposed model. As discussed in detail, in both cases the original salt load is replaced by an equivalent volume of (irreversibly) imbibed water. However, in the $CaSO_4$ depleted matrix, where no ZEH form, the cavities left behind by salt merely fill with water. In the NaCl-depleted matrix, we showed that (1) the said cavities partially collapsed and (2) the remaining additional (irreversibly) imbibed water is more homogeneously distributed in the matrix. The first effect is consistent with the expected higher mobility of the macromolecules at the cavity wall induced by ZEH formation; the second effect implies incomplete final collapse of the ZEH, in line with the substantial absorption–desorption hysteresis exhibited by the CA–water system (amply demonstrated in Roussis[9]).

A major part of the work reported here was performed under Contracts FI1W/0026/00 and FI1W/0174/GR(TT) as part of the European Community's Research Program on Management and Disposal of Radioactive Waste. Thanks are due to Mr. J. K. Petrou for taking charge of the computations.

REFERENCES

1. K. G. Papadokostaki, S. G. Amarantos, and J. H. Petropoulos, *J. Appl. Polym. Sci.,* **67,** 277 (1998).
2. T. Higuchi, *J. Pharm. Sci.,* **50,** 874 (1961).
3. J. H. Petropoulos, K. G. Papadokostaki, and S. G. Amarantos, *J. Polym. Sci., Polym. Phys.,* **30,** 717 (1992).
4. H. Yasuda, C. E. Lamaze, and L. D. Ikenberry, *Macromol. Chem.,* **118,** 19 (1968).
5. H. Yasuda, C. E. Lamaze, and A. Peterlin, *J. Polym. Sci., A2,* **9,** 1117 (1971).
6. K. C. Sung and E. M. Topp, *J. Controlled Release,* **37,** 95 (1995).
7. S. X. Chen and R. T. Lostritto, *J. Controlled Release,* **38,** 185 (1996).
8. (a) J. Crank, *The Mathematics of Diffusion,* 2nd ed., Clarendon Press, Oxford, U.K., 1975, Chap. 10; (b) J. Crank, *The Mathematics of Diffusion,* 2nd ed., Clarendon Press, Oxford, U.K., 1975, Chap. 4.
9. P. P. Roussis, *Polymer,* **22,** 768 (1981) and references therein.
10. P. I. Lee, in *Controlled Release Technology,* P. I. Lee and W. R. Wood, Eds., ACS Symposium Series 348, American Chemical Society, Washington, D.C., 1987, Chap. 5.
11. R. Gale, S. K. Chandrasekaran, D. Swanson, and J. Wright, *J. Membr. Sci.,* **7,** 319 (1980).
12. J. Wright, S. K. Chandrasekaran, R. Gale, and D. Swanson, *AIChE Symp. Ser.,* **206,** 62 (1981).
13. N. Narkis, M. Narkis, and I. Berkovitz, *J. Appl. Polym. Sci.,* **27,** 1795 (1982).
14. R. Schirrer, P. Thepin, and G. Torres, *J. Mater. Sci.,* **27,** 3424 (1992).
15. B. G. Amsden, Y.-L. Cheng, and M. F. A. Goosen, *J. Controlled Release,* **30,** 45 (1994).
16. B. G. Amsden and Y.-L. Cheng, *J. Controlled Release,* **31,** 21 (1994).
17. P. I. Lee, *Polym. Commun.,* **24,** 45 (1983).
18. P. I. Lee and C.-J. Kim, *J. Controlled Release,* **16,** 229 (1991).
19. G. Di Colo, V. Campigli, V. Carelli, E. Nannipieri, M. F. Serafini, and D. Vitale, *Il Farmaco,* Ed. Pr., **39,** 310 (1984).
20. V. Carelli, G. Di Colo, C. Guerrini, and E. Nannipieri, *Int. J. Pharm.,* **50,** 181 (1989).
21. Y. H. Bae, T. Okano, C. Ebert, S. Heiber, S. Dave, and S. W. Kim, *J. Controlled Release,* **16,** 189 (1991).
22. M. E. Heyde, C. R. Peters, and J. E. Anderson, *J. Colloid Interface Sci.,* **50,** 467 (1975).
23. H. K. Lonsdale, U. Merten, and R. L. Riley, *J. Appl. Polym. Sci.,* **13,** 1341 (1965).
24. K. G. Papadokostaki and J. H. Petropoulos, *J. Polym. Sci., Polym. Phys.,* **32,** 2347 (1994).
25. R. W. Korsmeyer, S. R. Lustig, and N. A. Peppas, *J. Polym. Sci., Polym. Phys. Ed.,* **24,** 395 (1986).
26. P. Meares, *J. Polym. Sci.,* **27,** 405 (1958).
27. E. Drioli, L. Nicolais, and A. Cifferi, *J. Polym. Sci., Polym. Phys. Ed.,* **11,** 3327 (1973).
28. H. K. Lonsdale, in *Desalination by Reverse Osmosis,* U. Merten, Ed., MIT Press, Cambridge, MA, 1966, Chap. 4.
29. J. H. Petropoulos, *J. Membr. Sci.,* **18,** 37 (1984).
30. J. H. Petropoulos, *J. Polym. Sci., Polym., Phys. Ed.,* **22,** 183 (1984).